Journal of Solar Energy Research (JSER)

Journal homepage: jser.ut.ac.ir

The Effect of Climatic Conditions on the Performance of a New Configuration of Solar Chimney

Ali Salehi[a], Shahram Delfani[b], Maryam Karami[c,*], Mehran Bozorgi

[a]*Faculty of Architecture and Urban Planning, Tehran University of Art, Tehran, Iran*
[b]*Department of Mechanical and Electrical Installations, Road, Housing and Urban Development Research Center (BHRC), Tehran, Iran*
[c]*Faculty of Engineering, Kharazmi University, Tehran, Iran*
[d]*School of Mechanical Engineering, College of Engineering, University of Tehran, Tehran, Iran*

A B S T R A C T

In this study, a new configuration of the solar chimney is introduced and its performance is compared with the conventional one. Using numerical simulation, the effect of different climatic conditions (cold and dry, hot and arid, hot and humid) on the performance of the new solar chimney is studied using the weather information of three cities of Iran including Tabriz (cold and dry), Yazd (hot and arid), and Bandar Abbas (hot and humid). It is found that the new solar chimney has 13-20% better performance than the conventional one, depending on climatic conditions. Also, the results showed that the performance of the new configuration is better in cold and dry climate zone than that in the other zones. Additionally, in this study, a new correlation for the estimation of the mass flow rate of solar chimney is introduced using four non-dimensional parameters.

Keywords: Solar chimney; Natural ventilation; Climatic conditions; Non-dimensional analysis

1. Introduction

Increasing energy consumption of the building, especially for providing thermal comfort, has led to numerous researches on the energy-saving approaches [1]. Passive and active solar energy technologies have become a noteworthy component of the energy saving in sunny regions of the world [2-4] Passive cooling is an effective method in decreasing energy consumption and providing better thermal comfort conditions by comparison with forced ventilation [5]. A solar chimney (SC) is a well-known passive cooling system, which plays an important role in the design of energy-efficient building.

In recent years, a considerable number of researchers have investigated different aspects of SC [6,7]. Chen et al. [8] have conducted experimental studies on SC with variable chimney gap-to-height ratios between 1:15 and 2:5 and different heat fluxes and inclination angles. It is found that an increase of 45% in air flow rate is achieved at an inclination angle around 45˚ for a 200 mm gap and 1:5 m height chimney by comparison with a vertical SC with the same identical conditions. Experimental investigations have been carried out by Mathur et al. [9] proved that an increase in the ratio between the height of absorber and air gap increased the rate of ventilation of the absorber. . Hariss and Helwig [10] assessed the impacts of the inclination angle, double glazing and low-emissivity finishes on the induced ventilation rate of an SC and presented the optimum inclination angle of 67.5˚ for a

*corresponding author: Karami@khu.ac.ir

to a vertical SC. Amori and Mohammad [11] numerically and experimentally investigated an SC with different air entrance gates and displayed that an SC with a side entrance had a higher mass flow rate. Mahdavinejad et al. [12] investigated an SC in four cities of Iran by ENERGY PLUS software and showed that the maximum ventilation flow rate was obtained at 45˚. Larbi et al. [13] investigated SC numerically, showing that the ventilation mass flow rate depended on air flow temperature and velocity distributions along with the chimney.

Khanal and Lei [14] numerically investigated solar chimney and reported that the mean difference of the mass flow rate between attached and stand-alone types of SC was approximately 10%. Imran et al. [15] investigated a solar chimney experimentally and numerically in terms of inclination angle, the intensity of solar radiation as well as the air gap. Accordingly, they demonstrated that the maximum induced air flow rate occurred with a 60º angle, for a radiation intensity of 750 W/m^2 at an air gap of 50 mm. Asadi et al. [16] used ENERGY PLUS software to simulate and assess the layout of the SC in three different sides and consequently proved that the maximum flow rate provided in the east-southern side due to the maximum radiation.

Shi et al. [17] evaluated the previous numerical models, resulting from experimental studies of the SC in order to develop a general empirical model. Accordingly, they assessed eight different parameters that affect the mass flow rate of the SC, and so they proved that the air velocity increases with a larger height to the air gap, but the volumetric flow rate behaves oppositely. Hosein and Selim [18] developed a mathematical model predicting the performance of an SC by considering different geometrical and operational parameters. The results showed that the chimney gap and wind speed influence largely the air flow rate. Abdallah [19] investigated the impact of the thermal performance of an SC with a passive cooling wind tower on occupants' thermal comfort. The cooling device was integrated with the roof of a 30 m^2 test room. After monitoring the indoor condition within a 2 month period in summer, it was revealed that outlet air temperature from the wind tower was 27.3˚C, and also the calculated PMV was between -0.5 to +0.5. This work showed that the performance of the system can provide an acceptable thermal comfort condition for users during daytime in the climate of New Assiut, Egypt.

Optimization of solar chimney design, done by Cheng et al. [20], suggested a chimney configuration of 0.5 m high air inlet and 12.5 cm cavity depth. Using CFD simulation, Kong et al. [21] found that the optimum inclination angle of a roof-top solar chimney varies from 45° to 60°, depending on the latitude and season of operation. In an interesting work, Nguyen and Wells [22] investigated a solar chimney performance with a horizontal absorber surface. They reported that the flow rate of solar chimney increases by different parameters including the heat flux and length of the absorber surface, gap of the air channel, and height and width of the inlet and outlet sections.

The main focus of this study is to investigate the effect of the new proposed configuration of SC on its mass flow rate and energy savings using a thermosiphonic model. Moreover, there is a lack of awareness of how the climatic parameters have imapct on the thermal performance of SC. Therefore, the effect of climatic conditions on the SC performance for the natural ventilation of the case study building is investigated. The considered climate zones are cold and dry, hot and dry and hot and humid. Furthermore, in this study, the physical and climatic parameters are assessed to create groups of non-dimensional numbers for SC. An empirical correlation is presented to evaluate the relationship among the different parameters influencing the mass flow rate of an SC.

2. New configuration of solar chimney

Figure 3 indicates the design characteristics of conventional SC (SC1) [23] and the new proposed SC (SC2). The basic dimensions of both SCs are 3 m×6 m in height and length, respectively. Moreover, they have two hallow shaft-spaces, attached with a common reinforced concrete wall, acting as an absorber wall. The outside walls of the SCs are encompassed with insulation with a thickness of 10 cm. The only difference between SC1 and SC2 is that the outer concrete wall of SC1 is replaced with a metal surface in SC2 and also, the same volume of the wall is added to the absorber wall. The thickness of the absorber wall in SC2 is doubled; while, the thermal capacity of both SCs is kept constant. It is worth bearing in mind that the overall thickness (D) in SC1 is equivalence with the thickness of the absorber wall (d). However, the thickness of the absorber wall (d) is twice more than the overall thickness (D) in SC2.

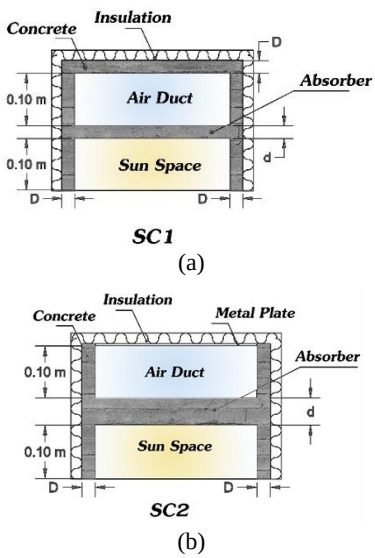

Figure 1. Horizontal cross section of (a) SC1 [19] (b) SC2

The SCs are equipped with air-dampers at the top and the bottom of each one, controlling air movement induced through the air duct between ambient and a residential house, shaped with a rectangular form, an open-plan with external sizes, length L = 10 m, width W = 7 m and height H = 3 m. The materials of the house walls, comprising heavy external walls from the outside layer to the inside layer, including 3cm cement veneer, 5cm thermal insulation, 10 cm brick and 2 cm gypsum and the roof, which consisted of the layers from outside to inside: mosaic, 5cm compacted thermal insulation of Polystyrene, 30 cm concrete slab and 3cm gypsum. The floor of the house was constructed on the ground composed of heavily reinforced concrete and covered with stone tiles. All of the external walls were assumed to be exposed to direct and indirect sunlight in which each had an opening equipped with a double glazed window and also overhang shadings with a length of 0.5 m; furthermore, the total area of four windows proven $10m^2$. The windows of the south, east and west facades were equipped with horizontal and vertical shadings whereas, the windows of the north façade had only vertical one and the façade equipped with a metal door. More details of the construction material properties are presented in Table 1.

Table 1. Construction material properties

Material	Solar absorptance	Visible absorptance	Thermal absorptance
Metal Surface (25 mm)	0.7	0.7	0.98
SC concrete	0.92	0.92	0.9
House concrete	0.7	0.7	0.9
Thermal insulation board			
Brick wall (100 mm)	0.1	0.1	0.9
Gypsum board (19 mm)			
Metal door	0.5	0.5	0.98
Mosaic	0.5	0.5	0.9
Cement board	0.1	0.1	0.9
Stone tiles	-	-	-

Material	Specific heat (J/kgK)	Thermal conductivity (W/mK)	Density (kg/m^3)
Metal Surface (25 mm)	418	45	7824
SC concrete	900	0.89	2050
House concrete	900	1.95	2240
Thermal insulation board	1210	0.03	43
Brick wall (100 mm)	790	0.89	1920
Gypsum board (19 mm)	1090	0.16	800
Metal door	418	45	7680
Mosaic	790	1.8	2560
Cement board	1000	0.58	1900
Stone tiles	790	3.17	2560

2-1 Climatic conditions

It is intended to choose three completely different climatic conditions to assess the impact of different climatic parameters on the thermal performance of SC; hence, three cities of Iran, as a multi-climate country, including Tabriz, Yazd, and Bandar Abbas were selected as seen in Figure 2. Tabriz, a city with cold and dry climate, located in the Northeast of Iran, its winter days are usually cold and snowy, while the summer is moderate. Yazd is located in the center of Iran, in the middle of a hot desert; thus, its climate is considered as hot and arid with hot diurnal hours, and cold nocturnal hours in summer. Bandar Abbas is placed in the south of Iran, beside the Persian Gulf; therefore, the rate of air humidity ratio is mostly high. Accordingly, its summer days are hot and humid, whereas its winter days are moderate [24]. Geographical characteristics and climatic conditions of the cities are presented in Table 2.

Figure 2. Location of three selected cities of the map of Iran

Table 2. Geographic and climatic conditions of the selected cities [25]

City	Longitude	Latitude	Climate	Altitude
Tabriz	45° 7′	36° 45′	Cold and Dry	1.35 m
Yazd	54° 24′	31° 54′	Hot and Dry	1.22 m
Bandar Abbas	52° 41′	25° 23′	Hot and Humid	3 m

3. Numerical simulation

Since the main goal of SC is to induce air movement associated with the stack effect to assist ventilation, ENERGY PLUS version 8.5.0. is chosen to perform a numerical simulation of SC. This software uses a TARP algorithm which is derived from the ASHRAE handbook (2001) providing equations for natural convection heat transfer coefficients in the turbulent range for large, vertical plates and for large, horizontal plates facing upward when heated (or descending when cooled), for evaluating the temperature distribution in the SC and hence, the thermal chimney module of ENERGY PLUS can simulate the thermal performance of SC by only considering the stack effect.

To validate the results of the simulation done by ENERGY PLUS, the thermosiphonic model of a full-size SC which It should be noted that the over-prediction and the under-prediction of the experimental results by the developed model could derive from the discrepancy between the real environmental situation on the days of the experimental study and the weather data files utilized in the transient simulation.

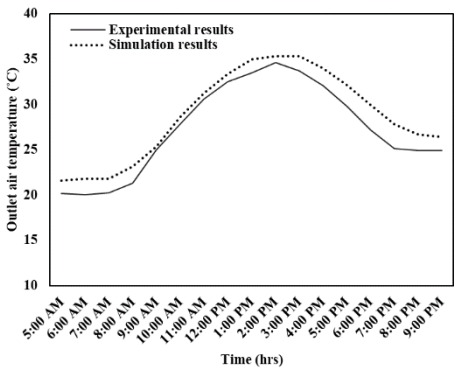

Figure 3. Variation of mean hourly SC outlet air temperature on September 15th

used in the experimental study done by Arce et al. [26], is developed in the software and the variations of three main parameters including outlet air temperature, absorber surface temperature and finally outlet air flow rate are compared with the experimental data [26, 27]. The experimental SC model is located in the desert of Tabernas, province of Almeria in southeastern Spain, with a hot and humid climate. The experimental model has a stand-alone position with two equal top and bottom openings, a concrete absorber wall with 1 m width, 0.15 m thickness and 0.30 m air gap. The geometry and physical details, as well as characteristics of the experimental model, were defined and incorporated into the settings of ENERGY PLUS 8.5.0 driven by information extracted from the studies done by Acre et al. [26] and Jiménez et al. [27].

As can be seen in Figure 3, a reasonable consistency exists between the calculated and measured mean hourly air temperature on September 15th [26], as the average deviation is around 5.5 %. Figure 4 illustrates a comparison between the calculated and measured absorber on October 9th [27]. It is also observed that the mean deviation is about 3%. Figure 5 illustrates the hourly variation of air mass flow rate obtained from the simulation and the experimental data [27] on December 28th. As can be seen in Figure 5, the compatibility between the calculated and measured results is acceptable between 5 AM to 12 PM at which the stack effect is dominant. The average deviation between 5 Am and 12 PM is approximately 6%.

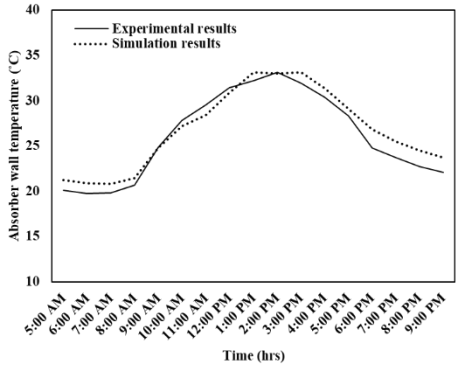

Figure 4. Variation of mean hourly SC absorber wall temperature on October 9th

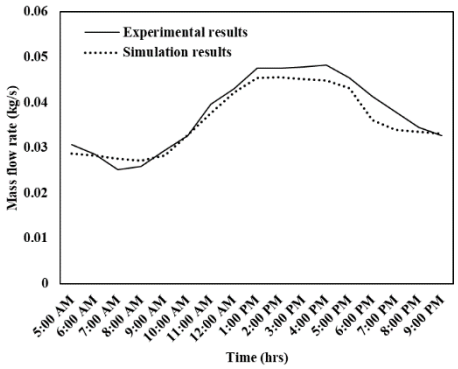

Figure 5. Variation of mean hourly SC mass flow rates on December 28th

3. Results and discussion

Figure 6 depicts the hourly variation of the outlet mass flow rate of SC1 and SC2 on July 15th. As observed, the hourly outlet air flow rate of SC2 is higher than SC1 in all three climate zones. The thermal performance of SC depends on the rate of harnessed solar energy. By increasing the amount of captured energy, the thermal performance of SC is improved. Since SC2 shows a higher amount of thermal mass exposure to solar radiation, the mass flow rate of SC2 is higher than that of the conventional SC. Figure 7 shows the average mass flow rate of SC1 and SC2 in three considered climate zones. As can be seen, the average mass flow rate of SC2 is 20%, 13%, and 18% higher than that of SC1 in cold and dry climate (Tabriz), hot and dry climate (Yazd) and hot and humid climate (Bandar Abbas), respectively. Considering the effect of the climatic conditions on the performance of SCs, it is also found from Figure 7 that the average mass flow rate of SCs is highest in Yazd because of the higher solar radiation in comparison with other climate zones, which is shown in Figure 8. However, the difference between the average mass flow rate in Yazd and Bandar Abbas is not too large, in spite of the significant higher solar radiation in Yazd by comparison with that in Bandar Abbas on the same day. This can be described considering the air humidity ratio and barometric pressure in these two cities. Based on the data presented in Figure 8, the humidity ratio is significantly high in Bandar Abbas by comparison with that in Yazd. It is obvious that the specific volume of air increases by increasing the humidity ratio. Consequently, the air density decreases, creating an updraft of air in the chimney. Therefore, the higher air humidity ratio in Bandar-Abbas than Yazd increases the mass flow rate of SC.

In addition, as indicated in Figure 9, the barometric air pressure is significantly higher in Bandar-Abbas than that in Yazd and Tabriz. By increasing the barometric air pressure, the stack effect enhances which results in the higher air temperature within the SC. Increasing the temperature causes the increase of the thermal expansion coefficient and thus, the Grashof number [28]; hence, the buoyancy force raises compared to the viscosity force, which leads to the enhancement of the mass flow rate of SC. Thus, the barometric air pressure, as well as the humidity ratio, can be considered as the factors that play a key role in the average of the mass flow rate of the SC.

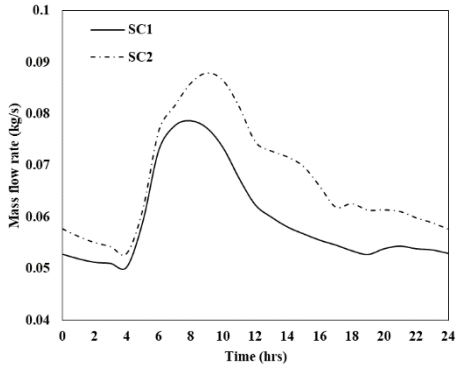

(a)

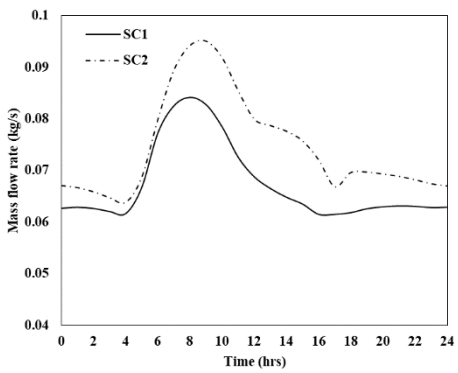

(b)

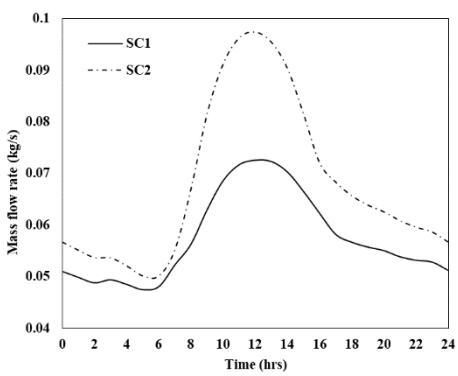

(c)

Figure 6. Hourly variation of mass flow rate of SC1 and SC2 in (a) Tabriz (b) Yazd (c) Bandar Abbas on July 15th

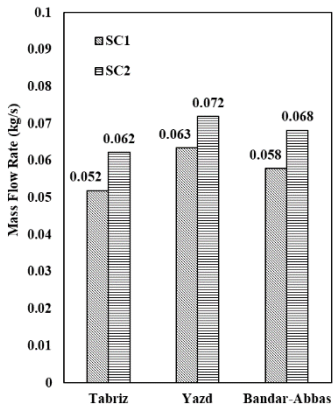

Figure 7. Average mass flow rate of SC1 and SC2 on July 15th

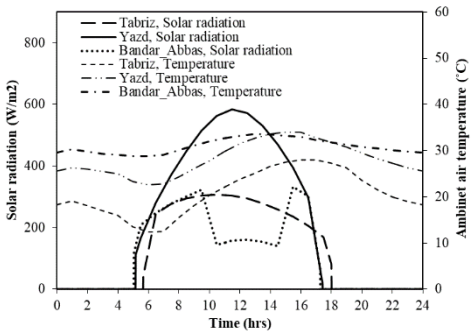

Figure 8. Variation of solar radiation and ambient air temperature on July 15th

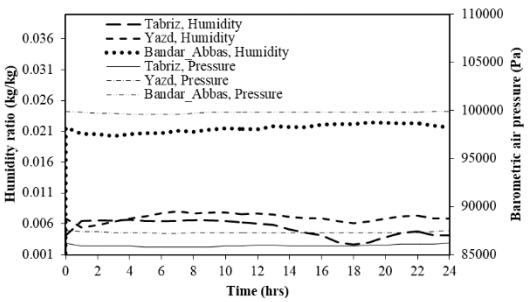

Figure 9 Variation of humidity ratio and barometric air pressure on July 15th

To find out the impact of SC on the reduction of energy consumption, the average space cooling load is calculated with and without SC2. The least zone infiltration rate was set at 0.2 ACH according to ASHRAE Standard 62.2 [29] in the case of without SC. However, for the space equipped with SC2, the zone infiltration depends on the performance of SC2. It is worth noting that the cooling load of Bandar Abbas is calculated on March 15th which has a moderate outdoor condition, while this condition occurs on June 15th for Tabriz and Yazd [30]. Figure 10 reveals that there is a significant difference between the average cooling load with and without SC2, in all considered climatic conditions. The average cooling load with SC2 is 6 times less than that without SC2 in Tabriz; whereas it is 10 times and 5 times less in Yazd and Bandar Abbas, respectively. It is concluded that that applying SC can have an extreme effect in reducing energy consumption in different climate zones.

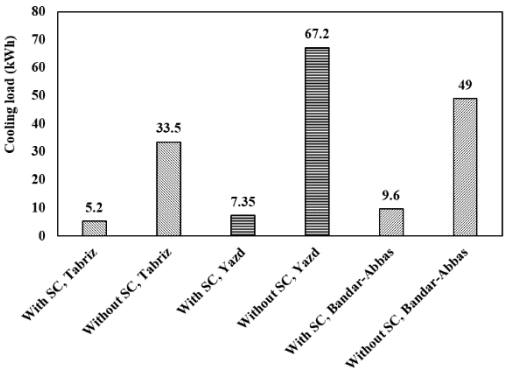

Figure 10. Average cooling loads with and without SC2

3.1. Non-dimensional analysis

To find out the parameters having a positive effect on the performance of SC, the impact of different physical and climatic parameters on the mass flow rate of SC is assessed using the non-dimensional analysis. A large number of parameters affect the mass flow rate of SC, as following:

$$\dot{m} = f\left(h, w, a, d, z, A_i, A_o, \theta, \alpha, v_{air}, T_i, T_o, R, G, C_p, \omega, P, g\right)$$

where f is a function which should be determined experimentally. In this study, Buckingham's theory [31] was applied to determine the groups of non-dimensional numbers. These groups are as follows:

$$\pi_1 = \frac{\dot{m}.g}{G.h} \quad (2)$$

$$\pi_2 = \frac{a.z.A_o}{w.h.\theta.A_i} \quad (3)$$

$$\pi_3 = \frac{P(gh)^{1.5}v_{air}\omega T_i}{G^2 T_o} \quad (4)$$

$$\pi_4 = \frac{GRC_p\alpha}{gd} \quad (5)$$

As shown, the non-dimensional numbers of π_1, π_2, π_3 and π_4 relates to the SC mass flow rate, the SC geometry, the environmental and climatic parameters and the SC absorber wall and materials, respectively.

To achieve the correlation between the different non-dimensional numbers and the mass flow rate [26, 27] including the most necessary physical, geometrical, and also the environmental data were utilized. The empirical correlation can be obtained using the Multiple Linear Regression Method as follows:

$$\pi_1 = (9.6E-11)\,\pi_3^{0.976}\pi_4^{0.964} \quad (6)$$

where the confidence coefficient is R2 = 97.5%.

Figure 11 is plotted to assess the empirical correlation achieved by the non-dimensional analysis. The horizontal axis shows the non-dimensional air mass flow rate resulted from the experimental data on September 15th [27], and the vertical axis shows the non-dimensional air mass flow rate obtained from the empirical correlation. As the slope of the fitted line is closer to one, the results are more accurate. In Figure 11, the line slope is 1.0049, verifying the precision of the proposed correlation.

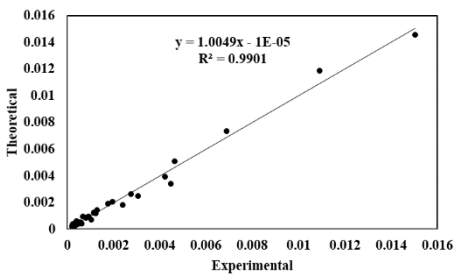

Figure 10. Comparing non-dimensional mass flow rate of SC calculated by empirical correlation and experimental results

To determine the deviation of the proposed correlation, the mass flow rate predicted using the correlation (π1) is compared with the experimental data taken from Hosein and Selim [18]. on October 9th. According to the data presented in Figure 12, there is a good agreement between the experimental and calculated data, confirming the accuracy of the correlation to predict the outlet mass flow rate of SC.

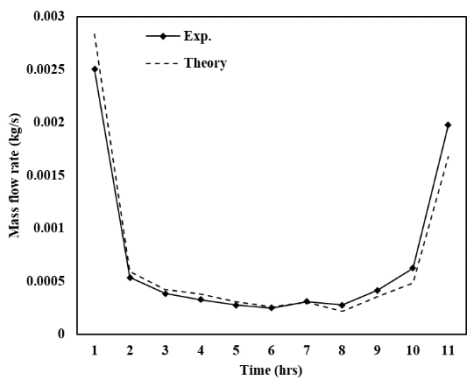

Figure 10. Comparison between the predicted and measured data [14]

The empirical correlation revealed that the mass flow rate of increases by increasing T_i,h,d 〖,v〗 _air, ω ,P, α and by decreasingR 〖,C〗 _p, 〖 T〗 _o. In general, the outdoor air velocity can be considered as a significantly effective factor, because it enhances the flow inside SC because of forced convection. It is also found that the solar radiation, the height and the absorption coefficient of the absorber wall can consolidate the stack effect, inducing the air flow inside the SC. Additionally, as was mentioned before, when the air humidity ratio increases, the air density decreases, which is useful for the induced air movement through SC.

Considering the results of the non-dimensional analysis, it is also proved that the better performance of SC2 than SC1 is because of decreasing thermal resistance of the outer wall in SC2, replacing the concrete wall with a metal surface. In addition, the findings properly coincide with the results, which indicate that the air humidity ratio and barometric pressure have a positive effect on the SC mass flow rate. It is worth noting that outdoor air temperature, which has a decreasing effect on the mass flow rate of SC, is higher in Bandar-Abbas (Figure 8) than that in two other cities. However, it appears that this parameter could not overweigh the effect of air pressure and air humidity ratio in Bandar-Abbas; therefore, the increasing impact of these parameters on the mass flow rate may be considered to be more than the decreasing impact of outdoor air temperature on the mass flow rate of SC.

4. Conclusion

In this study, a new configuration of the solar chimney (SC2) is developed and proved that SC2 provided a higher mass flow rate, ranging from 13% to 20%, depending on the climatic condition. The results proved that SC has a significant effect on the energy consumption reduction in different climates, ranging from 5 to 10 times less cooling load. For the first time, the physical and geometrical parameters, affecting on the mass flow rate of a vertical SC, are analyzed and consequently, a correlation for vertical SCs is presented using the non-dimensional analysis. As such, the non-dimensional analysis revealed that the increase of variables as inlet air temperature (Ti), the height of SC (h), the thickness of the absorber wall (d), absorbing coefficient of the absorber wall (α), air velocity (vair), barometric air pressure (P), and humidity ratio (ω), increase the mass flow rate, while the decrease of variables, such as thermal resistance (R), thermal capacity (Cp), and outdoor air temperature (To), increases the outlet mass flow rate of SC.

Acknowledgements

The authors would like to thank Dr. Ramin Rahmani, and Dr. Rima Fayaz for their useful comments, Eng. Pouya Bakhtiari for rewriting the weather data file, Dr. Sara Serahati for her statistical consultant on the non-

dimensional analysis, finally, Mahsa Haji-alibabaie as well as Mostafa Khodashenas for all their efforts on this work.

Nomenclature

a : Air gap of the sun space, m

Ai: Inlet area of SC, m2

Ao: Outlet area of SC, m2

Cp: Thermal capacity, J/K

d: Thickness of the absorber, m

D: General thickness of chimney, m

g: Gravitational acceleration, 9.81 m/s2

G: Solar irradiance, W/m2

$\dot{m}$: Mass flow rate, kg/s

P: Air barometric pressure, Pa

R: Thermal resistance of the system, m2.K/W

Ti: Inlet air temperature, K

To: Outlet air temperature, K

v_{air} : Velocity, m/s

w : Width of SC, m

z : The air gap of the air duct, m

Greek symbols

α : Absorption coefficient of the absorber wall

θ : Angle of SC with the horizontal axis, 90 degs

ω: Humidity ratio, kg of water vapor/m3 of dry air

References

1. Cao, X., Dai, X., Liu, J., *Building energy-consumption status worldwide and the state-of-the-art technologies for zero-energy buildings during the past decade*, Energy and Buildings, 2016. **128**: p. 198-213.

2. Xu, L., Luo, K., Ji, J., Yu, B., Li, Z., Huang, S., *Study of a hybrid BIPV/T solar wall system*, Energy, 2020. *193*: p.116578.

3. Karami, M., Javanmardi, F. (2020). Performance assessment of a solar thermal combisystem in different climate zone, Asian Journal of Civil Engineering, https://doi.org/10.1007/s42107-020-00236-0.

4. Karami, M., Asghari, B., Delfani, S., Akhavan-Behabadi, M.A., *Potential of nanodiamond/water nanofluid as working fluid of volumetric solar collectors*, Journal of Solar Energy Research, 2017. **2 (3)**: p. 71-78.

5. Yubin, Y., Li, H., Niu, F., Yu, D., *Investigation of a coupled geothermal cooling system with earth tube and solar*, Applied Energy, 2014. **114**: p. 209–217.

6. Jiménez-Xamán, C., Xamán, J., Moraga, N.O., Hernández-Pérez, I., Zavala-Guillén, I., Arce, J., Jiménez, M.J., *Solar chimneys with a phase change material for buildings: An overview using CFD and global energy balance*, Energy and Buildings, 2019. **186**: p. 384-404.

7. Vargas-López, R., Xamán, J., Hernández-Pérez, I., Arce, J., Zavala-Guillén, I., Jiménez, M.J., Heras, M.R., *Mathematical models of solar chimneys with a phase change material for ventilation of buildings: A review using global energy balance*, Energy, 2019. **170**: p. 683-708.

8. Chen, Z.D., Bandopadhayaya, P., Halldorssonb, J., Byrjalsenb, C., Heiselbergb, P., Lic, Y., *An experimental investigation of a solar chimney model with uniform wall heat flux*, Building and Environment, 2003. **38**: p.893 – 906.

9. Mathur, J., Bansal, N.K., Mathur, S., Jain, M., 2006, *Anupma, Experimental investigations on solar chimney for room ventilation*, Solar Energy, 2006. **80**: p. 927–935.

10. Harris, D.J., Helwig, N., *Solar chimney and building ventilation*, Applied Energy, 2007. **84**, p: 135–146.

11. Amori, K. E., Mohammed, S. W., *Experimental and numerical studies of solar chimney for natural ventilation in Iraq*, Energy and Buildings, 2012. **47**: p. 450–457.

12. Mahdavinejad, M., Fakhari, M., Alipoor, F., *The Study on Optimum Tilt Angle in Solar Chimney as a Mechanical Eco Concept*, Frontiers of Engineering Mechanics Research, 2013. **3**: p. 71-80.

13. Larbia, S., Hellaa, A. E., *Thermo-fluid aspect analysis of passive cooling system case using solar chimney in the south regions of Algeria*, Energy Procedia, 2013. **36**: p. 628 – 637.

14. Khanal, R., Lei, C., *A numerical investigation of buoyancy induced turbulent air flow inan inclined*

passive wall solar chimney for natural ventilation, Energy and Buildings, 2015. **93**: p. 217–226.
15. Imran, A. A., Jalil, J. M., Ahmed, S. T., *Induced flow for ventilation and cooling by a solar chimney*, Renewable Energy, 2015. **78**: p. 236-244.
16. Asadi, S., Fakhari, M., Fayaz, R., Mahdaviparsa, A., *The effect of solar chimney layout on ventilation rate in buildings*, Energy and Buildings, 2016. 123: p. 71–78.
17. Shi, L., Zhang, G., Cheng, X., Guo, Y., Wang, J., Chew, M. Y. L., *Developing an empirical model for roof solar chimney based on experimental data from various test rigs*, Building and Environment, 2016. **110**: p.115-128.
18. Hosein, M. A., Selim, S. M., *Effects of the geometrical and operational parameters and alternative outer cover materials on the performance of solar chimney used for natural ventilation*, Energy and Buildings, 2017. 138: p.355–367.
19. Abdallah, A.S.H., A new design of passive air condition integrated with solar chimney for hot arid region of Egypt, International Journal of Environmental Science and Technology, (2018).
20. Cheng, X., Shi, L., Dai, P., Zhang, G., Yang, H., Lib, J., *Study on optimizing design of solar chimney for natural ventilation and smoke exhaustion*, Energy and Buildings, 2019. 170: p. 145-156.
21. Kong, J., Niu, J., Lei, C., *A CFD based approach for determining the optimum inclination angle of a roof-top solar chimney for building ventilation*, Solar Energy, 2020. 198: p.555-569.
22. Nguyen, Y.Q., Wells, J.C., *A numerical study on induced flowrate and thermal efficiency of a solar chimney with horizontal absorber surface for ventilation of buildings*, Journal of Building Engineering, 2020. 28: Article number 101050.
23. Koronaki, I.P., *The impact of configuration and orientation of solar thermosyphonic systems on night ventilation and fan energy savings*, Energy and Buildings, 2013. 57: p. 119–131.
24. Iran Meteorological Organization, http://www.irimo.ir/far/services/climate/793. Accessed May, 20, 2016.
25. ENERGY PLUS site, https://energyplus.net/weather.
26. Arce, J., Himénez, M.J., Guzmán, J.D., *Experimental study for natural ventilation on a solar chimney*, Renewable Energy, 2009. 34: p. 2928–2934.
27. Jiménez, M.J., Guzmán, J.D., Heras, M.R., Arce, J., Xamán, J.P., Alvarez, G., *Thermal performance of a natural ventilation system*, in: Proceedings of the ASME 4th International Conference on Energy Sustainability, Phoenix, AZ, USA, 2010. p. 329–336.
28. Bergman, T. L. , Lavine, A. S., Incropera, F. P., DeWitt, D. P. , *Fundamentals of Heat and Mass Transfer*, Wiley, 7th Edition, 2011.
29. ASHRAE Standard 62.2, *Ventilation and Acceptable Indoor Air Quality in Low-Rise Residential Buildings*, American Society of Heating, Refrigerating and Air, Conditioning Engineers, 2007. Atlanta, GA.
30. Heidarinejad, G., Delfani, S., Amin Zanganeh, M., Heidarinejad, M., *Thermal comfort*, First ed., BHRC Publication, 2008.
31. Fox, R.W., Mc Donald, A.T., Pritchard, P.J., *Introduction to fluid dynamic*, John Wiley& Sons.inc, 2010. p. 168-237.